Magnetocrystalline anisotropy in UMn_{2}Ge_{2} and related Mn-based actinide ferromagnets

David S. Parker, Nirmal Ghimire, John Singleton, J. D. Thompson, Eric D. Bauer, Ryan Baumbach, David Mandrus, Ling Li, and David J. Singh

Phys. Rev. B **91**, 174401 — Published 4 May 2015

DOI: 10.1103/PhysRevB.91.174401

Magnetocrystalline Anisotropy in UMn_2Ge_2 and Related Mn-based Actinide Ferromagnets

David S. Parker
Materials Science and Technology Division, Oak Ridge National Laboratory, 1 Bethel Valley Rd., Oak Ridge TN 37831-6056

Nirmal Ghimire, John Singleton, J.D. Thompson, and Eric D. Bauer
Los Alamos National Laboratory, Los Alamos, NM 87545

Ryan Baumbach
National High Magnetic Field Laboratory, Tallahassee, FL

David Mandrus
Department of Materials Science and Engineering, University of Tennessee, Knoxville, TN and
Materials Science and Technology Division, Oak Ridge National Laboratory, Oak Ridge, TN 37831-6056

Ling Li
Department of Materials Science and Engineering, University of Tennessee, Knoxville, TN

David J. Singh
Materials Science and Technology Division, Oak Ridge National Laboratory, Oak Ridge, TN 37831-6056

We present magnetization isotherms in pulsed magnetic fields up to 62 Tesla, supported by first principles calculations, demonstrating a huge uniaxial magnetocrystalline anisotropy energy - approximately 20 MJ/m^3 - in UMn_2Ge_2. This large anisotropy results from the extremely strong spin-orbit coupling affecting the uranium $5f$ electrons, which in the calculations exhibit a substantial orbital moment exceeding 2 Bohr magnetons. We also find from theoretical calculations that a number of isostructural Mn-actinide compounds are expected to have similarly large anisotropy.

Introduction. Uranium- $3d$ transition metal compounds present a wide range of behaviors, ranging from superconductivity in U_6Mn and U_6Fe[1], ferromagnetism with T_c above room temperature in UMn_2Ge_2[2], antiferromagnetism and heavy-fermion behavior in UNi_4B,[3], and the unexpected paramagnetism[4] in UMn_2. All these materials appear to present an interplay across energy scales, in particular in which the uranium spin-orbit coupling rivals and sometimes exceeds typical energy scales such as the crystal field splitting and electronic band width.

Intrinsic magnetic anisotropy arises from this spin orbit coupling. Therefore, one expects high anisotropy in actinide magnets. However, in practice the situation is much more complex, particularly for high Curie temperature materials. While the anisotropy comes from the orbital moment direction set by spin orbit and the crystal field, magnetic ordering is generally due to electron hopping. Therefore high ordering temperature materials have a greater tendency towards quenching of orbital moments, which then can reduce the anisotropy. The stronger hybridization of the $5f$ levels of the light actinides with ligand orbitals, relative to the $4f$ elements, leads to stronger crystal field effects and potentially higher ordering temperatures, but also again to higher bandwidth and orbital moment quenching. On the other hand, the stronger spin orbit greatly favors orbital moments and anisotropy.

In this work we report and discuss the experimental observation and theoretical predictions of a huge low-temperature magnetocrystalline anisotropy energy (MAE) of 20.6 MJ/m^3 in UMn_2Ge_2, which orders ferromagnetically above room temperature with a large magnetization amounting to ~ 6 μ_B per formula unit, or approximately 0.85 Tesla. This was found by our high field measurements to 62 T on oriented crystal samples. While such large anisotropies have previously been observed in certain rare-earth magnets such as $SmCo_5$, to our knowledge this is the largest value observed to date in an actinide ferromagnet. It arises from a magnetic coupling between the manganese *3d* and uranium *5f* states. Both the Mn and the U carry sizable spin moments which are coupled to each other and in the case of U strongly tied to the lattice via spin-orbit. The extremely strong spin-orbit coupling in uranium then induces a large orbital moment on the uranium atom, opposite to the spin moment as a consequence of Hund's rules, leading to the extremely large magnetic anisotropy. Large anisotropy in U-containing ferromagnets is not confined to UMn_2Ge_2; Ref. 5 suggests similar behavior for UCu_2Ge_2.

Experimental Results. Single crystals of UMn_2Ge_2 were grown from 3N purity elements in a molten Zn flux. The reaction ampoules were made by loading the elements into a 2 mL alumina crucible in the ratio 1(U):2(Mn):2(Ge):20(Zn). The crucible was sealed under vacuum in a quartz tube, heated to 600 C over eight hours, held at 600 C for six hours, heated to 1050 C over six hours, held at this temperature for 24 hours, and then cooled to 650 C over 200 hours. After removing the flux by spinning the ampoules in a centrifuge, single crystal platelets with typical dimensions of several millimeters on a side and 0.5 - 1 millimeter thickness were collected.

As confirmed by x-ray diffraction, UMn_2Ge_2 crystallizes in the tetragonal $ThCr_2Si_2$ (or 122) structure with a planar lattice constants of 3.968 Å and c-axis lattice parameter 10.71 Å[6].

As we will see, experimentally the moments lie parallel to the c-axis and our calculations confirm this.

In Fig. 1 we show the electrical resistance data normalized to the value at $T = 400$ K ($R_{\rm NORM} = R/R(T = 400\ {\rm K})$) versus temperature T, where the electrical current was applied in the ab-plane. For $T > 360$ K, $R_{\rm NORM}$ increases gradually with decreasing T. Many related U-based compounds that crystallize in the $ThCr_2Si_2$ structure exhibit similar behavior (e.g., URu_2Si_2[7,8]) due to Kondo driven hybridization between the conduction- and f-electron states. At the manganese ordering temperature $T_{\rm C,Mn} \approx 360$ K, $R_{\rm NORM}$ undergoes a decrease that is consistent with a second order phase transition into the ordered state (right inset), and subsequently decreases gradually with decreasing T. Although magnetization, neutron scattering, and Kerr effect measurements reveal ferromagnetic ordering of the uranium ions near $T_{\rm C,U} \approx 150$ K[9–11], we do not observe any corresponding change in $R_{\rm NORM}$, as we did not perform these more magnetization-sensitive measurements in this temperature range. Finally, we find that $R_{\rm NORM}$ goes through a minimum near 12 K and then moderately increases to the lowest T measured (left inset). The low temperature upturn is similar to what is seen for an effective single ion Kondo effect.

The likely Kondo physics apparent in the resistivity upturn below 12 K is somewhat reminiscent of URu_2Si_2,[12–16] which exhibits a substantial Kondo effect, with a Kondo temperature[17] of several hundred Kelvin. In UMn_2Ge_2, however, we estimate a much smaller Kondo temperature of order 1 K, which is roughly consistent with the 10 K value obtained from the upturn of the very low-temperature resistance, considering the exponential dependence of T_K. Similarly, we also estimate an RKKY temperature T_{RKKY} (presumably linking the U $5f$ spins and the Mn conduction electrons)[18,19] for UMn_2Ge_2 as approximately 10 K. The Kondo and RKKY temperatures in UMn_2Ge_2 are therefore three or more orders of magnitude smaller than the spin-orbit coupling responsible for the magnetocystalline anisotropy.

In Fig. 2 we show heat capacity C_P vs. temperature data, where C_P/T decreases monotonically with decreasing T over most of the measured temperature range. For $2 < T < 20$ K we fit the data (inset) using the expression $C/T = \gamma + \beta T^2$, where $\gamma = 31$ mJ/molK^2 is the electronic contribution and $\beta = 0.22$ mJ/molK^4 is the coefficient of the phonon term, which gives a Debye temperature ($\Theta_{\rm D} = 353$ K). From γ, we infer that weak quasiparticle mass enhancement exists inside the ordered state. Below $T = 2$ K, C/T undergoes a minor increase with decreasing T, which may signal the onset of a nuclear Schottky anomaly.

The pulsed-field magnetization experiments used a 1.5 mm bore, 1.5 mm long, 1500-turn compensated-coil susceptometer, constructed from 50 gauge high-purity copper wire[20]. When a sample is within the coil, the signal is $V \propto ({\rm d}M/{\rm d}t)$, where t is the time. Numerical integration is used to evaluate M. Samples were mounted within a 1.3 mm diameter ampoule that can be moved in and out of the coil. Accurate values of M are obtained by subtracting empty-coil data from that measured under identical conditions with the sample present. The susceptometer is calibrated by scaling low-field M values to match those recorded with a sample of known mass measured in a commercial SQUID or vibrating-sample magnetometer.

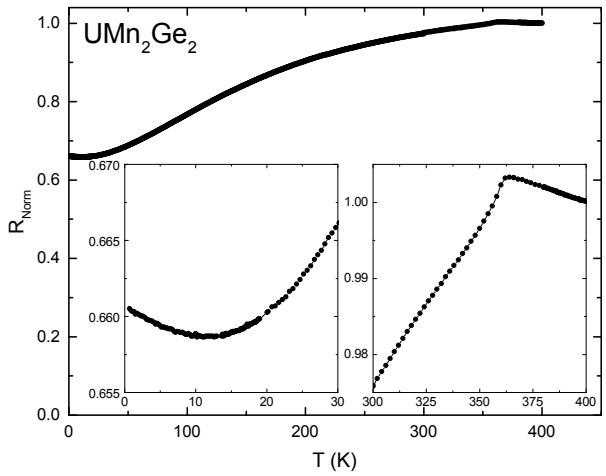

FIG. 1. Electrical resistance data normalized to the value at $T = 400$ K $R_{\rm NORM} = R/R(T = 400\ {\rm K})$ versus temperature T for UMn_2Ge_2. Left inset: Low temperature region of $R_{\rm NORM}(T)$ showing the weak upturn for $T < 13$ K. Right inset: $R_{\rm NORM}(T)$ in the region surrounding the Mn ferromagnetic ordering temperature $T_{\rm C,Mn} \approx 360$ K.

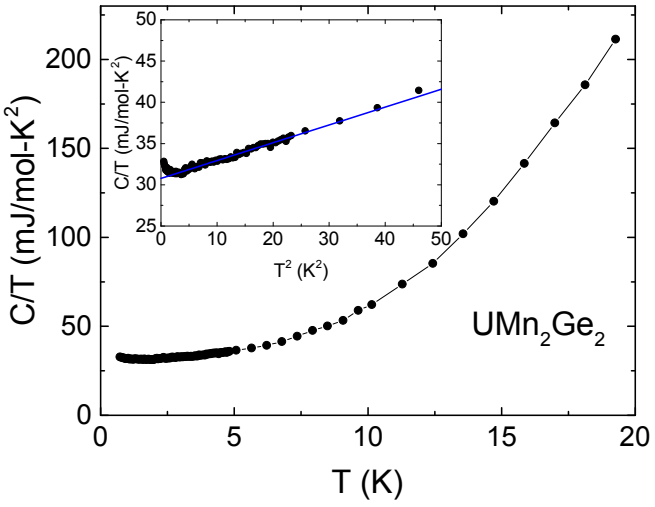

FIG. 2. Heat capacity divided by temperature C/T vs T for UMn_2Ge_2. Inset: C/T vs T^2. The solid line is a fit to the data, as described in the text.

Fields were provided by a 65 T short-pulse magnet at NHMFL Los Alamos. The susceptometer was placed within a ^{3}He cryostat providing Ts down to 0.4 K. B was measured by integrating the voltage induced in a ten-turn coil calibrated by observing the de Haas-van Alphen oscillations of the belly orbits of the copper coils of the susceptometer[20]. Figure 3

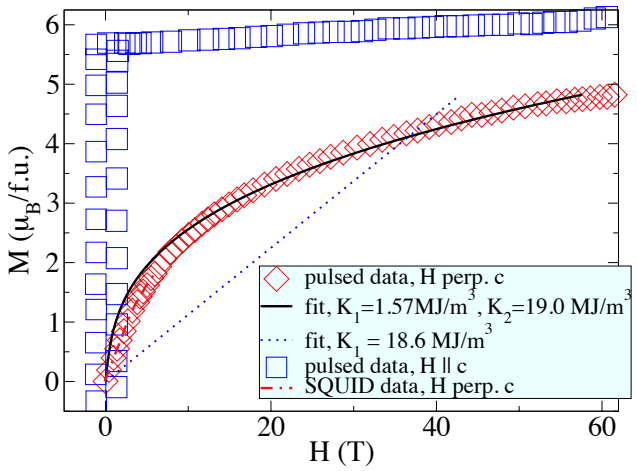

FIG. 3. The results of pulsed-field measurements of the magnetic anisotropy on axially aligned single crystals of UMn_2Ge_2. The purple lines represent the response for the field parallel to the easy-axis (c-axis), and the black line for **H** applied in the plane. The red line shows SQUID measurements made at lower fields.

depicts the results of the pulsed field measurements. For **H** in the easy-axis c direction, there is a rapid saturation of the magnetization, reaching nearly 6 μ_B per formula unit for a field of less than 2 Tesla and then increasing very slowly up to about 6.15 μ_B /f.u. at 62 Tesla. There is some hysteresis observed in the data, which may reflect granular microstructure in the sample. For **H** in the planar direction, the situation is very different. Although the magnetization increases rapidly at first, reaching 2 μ_B at roughly 5 Tesla, thereafter it rises much more slowly and is not near saturation even at 62 Tesla, the limit of the measurement. The strong curvature of $M(H)$ suggests unusual anisotropy behavior, apart from simply the large magnitude of the anisotropy. For a tetragonal material such as UMn_2Ge_2, the magneto crystalline anisotropy energy (MAE) can be written in the form

$$E(\theta) = E_0 + K_1 \sin^2(\theta) + K_2 \sin^4(\theta) + ... \qquad (1)$$

where θ is the polar angle of moment orientation relative to the c-axis. For K_1 and K_2 positive, the material is uniaxial.

Ordinarily one observes a K_2 much smaller than K_1 (We neglect the higher order azimuthal term since we do not know the samples' azimuthal orientation). One then extracts the field dependence of the magnetization by minimizing the total system energy with respect to polar angle, including the magnetostatic term $\mathbf{M}\cdot\mathbf{H}$; an explicit expression for this is found in Ref.[21]. However, the best fit has a K_2 *more than ten times larger* than K_1 - quantitatively, the values are 19.0 MJ/m^3 and 1.57 MJ/m^3, respectively. It is difficult to understand the reason for this behavior. Note that one can fit the data (not shown), albeit with degraded high-field agreement, by constraining K_1 to fit the low-field M vs. H slope, in which case K_2 is found as approximately three times K_1. In Figure 3 we also show a fit with K_2 constrained to zero - the results necessarily follow a straight line. The great curvature of the best-fit line is specifically due to the size of K_2 relative to K_1. While the relative magnitude of the anisotropy constants is highly unusual, it is not unknown in actinide compounds; Ref.[22] presents a similar scenario for U_3As_4. The value of the anisotropy field inferred from the fit is 117 Tesla.

One may check these fit values for self-consistency. Another method of determining the anisotropy energy is simply to measure the area between the magnetization curves for the field in-plane and axial. Neglecting other stresses on the crystal, this area represents the magnetic work necessary to change the orientation of the moments from axial to planar. The high field behavior of M(H) for H in the plane is assumed to be linear up to the anisotropy field. This method gives a total anisotropy energy of 21.8 MJ/m^3, which is within 6 percent of the value from the fit.

First principles calculations. An extremely large anisotropy is found in first principles results, which predicted this prior to the measurements. First principles calculations, using the linearized augmented plane wave (LAPW) code WIEN2K[23] and the generalized gradient approximation (GGA) of Perdew *et al*[24] were performed, with an RK_{max} of 9 and necessarily including spin-orbit coupling. Sphere radii of 2.5 Bohr for Uranium and 2.29 Bohr for Manganese and Germanium were used, with up to 10000 k-points in the full Brillouin zone used for magnetic anisotropy calculations. The calculated magnetic moment was 3.95 μ_B per unit cell, including an orbital contributions of 2.01 μ_B from the Uranium and 0.08 μ_B from each Manganese.

Given the notable difficulties in modeling the actinides from first principles, we do not expect complete agreement with experiment, and our calculated moment is significantly lower than the 6.15 μ_B per formula unit we observe, and our calculated MAE of 36.0 MJ/m^3 is substantially larger than the experimental value. We find the ground state to have the Uranium spin moment opposite to that of the Manganese, with an energy penalty relative to U-Mn ferromagnetic alignment of 140 meV per formula unit, indicating a U-Mn exchange coupling J_{U-Mn} of some 8.5 meV. Such an exchange coupling is perhaps somewhat surprising, given the large U-Mn nearest neighbor distance of some 3.33 $\AA$. This energy scale is, however, comparable to the approximate 150 K ordering temperature[2] of the Uranium atoms, suggesting the importance of the Manganese interaction for the Uranium magnetic behavior.

The calculated T-linear bare specific heat coefficient γ_0 (spin-up and spin-down contributions summed) is 16.7 mJ/mol-K^2). When this is compared to the experimental value γ from Fig. 2 of 31 mJ/mol-K^2, using $\gamma = \gamma_0(1+\lambda)$ one finds a a quasiparticle mass enhancement λ of 0.9. Note that γ_0 computed for planar moments (in fact, the 110 direction) is 11.1 mJ/mol K^2, or forty percent less. This suggests a spin-orbit scale comparable to the crystal field.

We do not report here GGA+U calculations appropriate to consideration of electron correlation since the light actinides, including Uranium, are not typically regarded as strongly

correlated; indeed, recent work[25] has shown that the LDA and GGA provide good descriptions of the properties of Uranium.

Discussion. To explain the observed magnetic properties of UMn_2Ge_2, in Table 1 we present structural and calculated magnetic results for UMn_2Ge_2, UMn_2Si_2, and UMn_2, which we argue represent different degrees on the local moment-itinerant behavior continuum. Note that for UMn_2 we have used the experimentally observed orthorhombic low-temperature structure[26], rather than the more well-known fcc structure. The plots depict a steady decrease in the size of the spin moments on the Mn and U sites as the respective Mn-Mn and U-U distances decrease. The U spin moment decreases by some 11 percent from UMn_2Ge_2 to UMn_2Si_2 despite a change in nearest neighbor U-U distance of just -0.05 Å. If extrapolated linearly this would yield a nil U moment for a U-U distance of approximately 3.5 Å, which would fall in line with the Hill criterion[27] , which asserts that U atoms order for U-U nearest neighbor distances of 3.5 Å or greater. With a U-U distance of 3.97 Å in UMn_2Ge_2, we argue that the U moments are substantially localized. Supporting this assertion are the separate ordering temperatures of the U and Mn ions as observed previously by neutron diffraction, with the Mn atoms ordering at approximately 360 K but the U atoms ordering at a much lower temperature of approximately 150 K.

TABLE I. Nearest-neighbor distances and calculated spin moments M_S of three Uranium Manganese materials.

Compound	Mn $M_S(\mu_B)$	Mn-Mn dist. (Å)	U M_S	U-U dist.
UMn_2Ge_2	2.10	2.81	-1.93	3.97
UMn_2Si_2	1.89	2.77	-1.72	3.92
UMn_2	1.55*	2.41,2.53	-1.11	2.92,3.26

*Average of two inequivalent Mn sites in orthorhombic structure.

A related criterion for Mn[27] argues that Mn atoms order magnetically for Mn-Mn distances above 2.7 Å. We see that both ferromagnetic U-Mn 122 compounds have nearest neighbor Mn distances above this value, with a 10 percent decrease in Mn spin moment as the Mn-Mn nearest neighbor distance decreases from 2.81 to 2.77 Å.

Interestingly, the *calculated* results for UMn_2, while agreeing with the trend of decreasing moment magnitudes with decreasing nearest neighbor distances, are apparently at odds with the *experimental* situation[28], which does not find magnetic order in this compound. We ascribe this inconsistency to the well-known difficulties that actinide compounds present to first principles calculations. The U-U nearest neighbor distances in this structure are substantially below the Hill criterion value, suggestive of a non-magnetic state. The magnetism found theoretically has itinerant character as opposed to the local character in UMn_2Ge_2.

Comparison of the three materials suggests that the Ge atoms in UMn_2Ge_2 provide spacers for the U and Mn atoms so that these atoms can form sizable local moments; these moments are much larger than those calculated for the UMn_2 compound.

Since we anticipate that other 122 structure manganese actinide ferromagnets might also exhibit similarly large magnetocrystalline anisotropy, we present in Table 2 calculated anisotropy energies for several such Mn 122 ferromagnets, including UMn_2Ge_2. All anisotropies are large and uniaxial, and are remarkably similar in magnitude. Note however that electron correlations become more important as the atomic number increases in the actinide series. For example, the metallic elements up to Np are generally viewed as itinerant f-systems, Pu as a cross-over material and those above Pu as localized. It is likely that the 122 structure is itself conducive to large anisotropy due to the relatively low symmetry of the actinide site. We expect that large anisotropies would likely be found experimentally in these other 122 compounds if tested.

TABLE II. The calculated magnetic anisotropy ($\Delta E = E_{100}$-E_{001}) of several Mn 122 actinide ferromagnets.

Compound	$\Delta E(MJ/m^3)$
UMn_2Si_2	31.4
UMn_2Ge_2	36.0
$NpMn_2Si_2$	29.2
$NpMn_2Ge_2$	31.0

To summarize, we have shown experimentally that the 122 structure ferromagnetic manganese actinide compound UMn_2Ge_2 has a huge axial magnetocrystalline anisotropy, found as 20.6 MJ/m^3 from pulsed magnetic field measurements at the NHMFL. First principles calculations support this finding and predict large anisotropies in several other Mn-based 122 actinide ferromagnets, suggesting that large anisotropy may be an intrinsic feature of this structure when magnetic actinides are present.

Acknowledgments Work at Oak Ridge National Laboratory was supported by the Critical Materials Institute, an Energy Innovation Hub funded by the U.S. Department of Energy, Energy Efficiency and Renewable Energy, Advanced Manufacturing Office (D.P.), and by the U.S. DOE, Office of Science, Basic Energy Sciences, Materials Science and Engineering, Division (DM and DJS). Work at Los Alamos National Laboratory was performed under the auspices of the U.S. DOE, OBES, Materials Science and Engineering. DM and LL acknowledge support from NSF DMR-1410428.

[1] H.H. Hill and B.T. Matthias, Phys Rev. **168**, 464 (1968).

[2] A.J. Dirkmaat, T. Endstra, E.A. Knetsch, A.A. Menovsky, G.J. Nieuqenhuys and J.A. Mydosh, J. Mag. Mag. Mat. **84**, 143 (1990).

[3] R. Movshovich, M. Jaime, S. Mentink, A.A. Menovsky and J.A. Mydosh, Phys. Rev. Lett. 83, 2065 (1999).

[4] A.M. Boring, R.C. Albers, G.H. Schadler, A.C. Lawson, P. Weinberger and N.E. Christensen, Phys, Rev. B **36**, 5507 (1987).

[5] T. D. Matsuda, S. Ikeda, E. Yamamoto, Y. Haga, and Y. Onuki, J. Phys. Soc. Jpn. **76**, 074708 (2007).

[6] R. S. Chaughule, R.J. Begum, R. Nagarajan, L.C. Gupta, R. Vijayaraghavan, A.D. Kulkarni, P. Rai, P. Suryanarayana, A. Sathyamoorthy and K. Shashikala, J. All. Comp. **178**, 385 (1992).

[7] W. Schlabitz, J. Baumann, B. Pollit, U. Rauchschwalbe, H. M. Mayer, U. Ahlheim, and C. D. Bredl, Z. Phys. B **62**, 171 (1985).

[8] M. B. Maple, J. W. Chen, Y. Dalichaouch, T. Kohara, C. Rossel, M. S. Torikachvili, M. W. McElfresh, and J. D. Thomspon, Phys. Rev. Lett. **56**, 185 (1986).

[9] A. Szytula, S. Siek, J. Leciejewicz, A. Zygmunt, and Z. Ban, J. Phys. Chem. Solids **49**, 1113 (1988).

[10] P. P. J. van Engelen, D. B. de Mooij, and K. H. J. Buschow, IEEE Transactions on Magnetics **24**, 185 (1988).

[11] R. D. Kirby, J. X. Shen, J. A. Woollam, and D. J. Sellmyer, J. Appl. Phys. **69**, 4574 (1991).

[12] J. Schoenes, C. Schonenberger, J.J.M. Franse and A.A. Menovsky, Phys. Rev. B **35**, 5375 (1987).

[13] S. Elgazzar, J. Rusz, M. Amft, P.M. Oppeneer and J.A. Mydosh, Nat. Mat. **8**, 337 (2009).

[14] A.R. Schmidt, M.H Hamidian, P. Wahl, F. Meier, A.V. Balatsky, J.D. Garrett, T.J. Williams, G.M Luke and J.C. Davis, Nature **465**, 570 (2010).

[15] R. Okazaki, T. Shibauchi, H.J. Shi, Y. Haga, T.D. Matsuda, E. Yamamoto, Y. Onuki, H. Ikeda and Y. Matsuda, Science **331**, 439 (2011).

[16] P. Chandra, P. Coleman and R. Flint, Nature **493**, 621 (2013).

[17] K. Sugiyama, H. Fuke, K. Kindo, K. Shimohata, A.A. Menovsky, J.A. Mydosh and M. Date, J. Phys. Soc. Jpn. **59**, 3331 (1990).

[18] M.A. Ruderman and C. Kittel, Phys. Rev. **96**, 99 (1954).

[19] E. Hassinger, *Competition of ground states in URu_2Si_2 and UCoGe*; Ph.D. thesis, Universite de Grenoble, 2010; available from https://tel.archives-ouvertes.fr/tel-00533732.

[20] P. A. Goddard, J. Singleton, P. Sengupta, R. D. McDonald, T. Lancaster, S. J. Blundell, F. L. Pratt, S. Cox, N. Harrison, J. L. Manson, H. I. Southerland and J. A. Schlepper, New J. Phys. **10** 083025 (2008).

[21] H.J. Williams, R.C. Sherwood and O.L. Boothby, J. Appl. Phys. **28**, 445 (1957).

[22] V.E. Bril, R.Z. Levitin, R.E. Osipova, V.L. Yakovenko and M. Zeleny, Phys. Stat Sol A **57**, 393 (1980).

[23] P. Blaha, K. Schwarz, G. K. H. Madsen, D. Kvasnicka and J. Luitz, WIEN2k, An Augmented Plane Wave + Local Orbitals Program for Calculating Crystal Properties (Karlheinz Schwarz, Techn. Universität Wien, Austria), 2001. ISBN 3-9501031-1-2.

[24] J. P. Perdew, K. Burke, and M. Ernzerhof, Phys. Rev. Lett. **77**, 3865 (1996); **78**, 1396 (1997).

[25] A.N. Chantis, R.C. Albers, M.D. Jones, M. van Schilfgaarde and T. Kotani, Phys. Rev. B **78**, 081101 (2008).

[26] A.C. Lawson, Jr., J.L. Smith, J.O. Willis, J.A. O'Rourke, J. Faber and R.L Hitterman, J. Less Com. Met. **107**, 243 (1985).

[27] K.V. Gurtovoi and R.Z. Letivin, Usp. Fiz. Nauk **153**, 193 (1987).

[28] S. Giri, H. Nakamura and M. Shiga, Phys. Rev. B **61**, 12233 (2000).